

**IDAHO DEPARTMENT OF FISH AND GAME**

**Ed Schriever, Director**

**Project F15AF00001 Amd 3**

**Evaluation of Camera-Based Occupancy Modeling for Estimating Ungulate Abundance**

**Final Report**



Performance Period  
October 1, 2014 through June 30, 2019

Compiled and edited by: Shane Roberts

September 2019  
Boise, Idaho

Idaho Department of Fish and Game (IDFG) adheres to all applicable state and federal laws and regulations related to discrimination on the basis of race, color, national origin, age, gender, disability or veteran's status. If you feel you have been discriminated against in any program, activity, or facility of IDFG, or if you desire further information, please write to: Idaho Department of Fish and Game, PO Box 25, Boise, ID 83707 or US Fish and Wildlife Service, Division of Wildlife and Sport Fish Restoration Program, 5275 Leesburg Pike, MS: WSFR, Falls Church, VA 22041-3803, Telephone: (703) 358-2156.

Findings in this report are preliminary in nature and not for publication without permission of the Director of the Idaho Department of Fish and Game.

Please note that IDFG databases containing this information are dynamic. Records are added, deleted, and/or edited on a frequent basis. This information was current as of the date of this report. Raw data do not have the benefit of interpretation or synthesis by IDFG.

IDFG requests that you direct any requests for this information to us rather than forwarding this information to third parties.

This publication will be made available in alternative formats upon request. Please contact IDFG for assistance.

## **FEDERAL AID IN WILDLIFE RESTORATION ANNUAL PERFORMANCE REPORT**

### **Need**

Animal abundance and age and sex ratios are important parameters for informing ungulate population dynamics. The Idaho Department of Fish and Game (IDFG) relies heavily on these estimates to both provide direct management information and to help inform population dynamics models. Yet, established methods for estimating abundance and age and sex ratios rely heavily on the use of helicopters with high observer visibility. These helicopters are becoming less available and more expensive resulting in frequent logistical constraints for obtaining abundance estimates. Therefore, it is important to identify and test alternative methods for estimating ungulate abundance, informing population models and tracking trends.

### **Purpose**

This project will test a camera-based occupancy estimation method that exploits the steep side of the occupancy-abundance relationship curve to estimate ungulate abundance. We will examine critical components of grid cell size, habitat relationships and camera distribution to help estimate abundance. The result will provide the Idaho Department of Fish and Game with a statistically rigorous and field-tested evaluation of occupancy as a metric to inform ungulate population management. This amendment will develop the final step from theory and model development to sampling design for implementing surveys to estimate abundance, survival, and age and sex ratios for population management activities.

### **Measurable Objective(s)**

1. Develop univariate relationships between design variables and precision
2. Develop univariate relationships between design variables and cost
3. Develop cost: precision tradeoffs.
4. Develop multi-factor relationships for cost: precision tradeoffs

### **Expected Results and Benefits**

Evaluate whether camera-based occupancy modeling is an efficient and effective monitoring tool for generating ungulate abundance information useful for management purposes.

**If the work in this grant was part of a larger undertaking with other components and funding, present a brief overview of the larger activity and the role of this project.**

N/A

**Describe how objectives were met:**

See Approach and Results sections below.

**Discuss differences between work anticipated in grant proposal and grant agreement, and that actually carried out with WSFR grant funds; include differences between expected and actual costs**

N/A

**List any publications or in-house reports resulting from this work**

Moeller, A. K., P. M. Lukacs, and J. S. Horne. 2018. Three novel methods to estimate abundance of unmarked animals using remote cameras. *Ecosphere* 9(8):e02331. 10.1002/ecs2.2331

Tabak, M. A., M. S. Norouzzadeh, D. W. Wolfson, S. J. Sweeney, K. C. Vercauteren, N. P. Snow, J. M. Halseth, P. A. Di Salvo, J. S. Lewis, M. D. White, B. Teton, J. C. Beasley, P. E. Schlichting, R. K. Boughton, B. Wight, E. S. Newkirk, J. S. Ivan, E. A. Odell, R. K. Brook, P. M. Lukacs, A. K. Moeller, E. G. Mandeville, J. Clune, and R. S. Miller. 2018. Machine learning to classify animal species in camera trap images: applications in ecology. *Methods in Ecology and Evolution* 2018:1-6. 10.1111/2041-210X.13120

**Approach**

From FY15-FY17, we examined existing telemetry data to determine a useful grid cell size. We considered ungulate home range size within the likely sampling period, movement rates within the home range, and use of different vegetation types. We targeted a grid cell size that contains a small number of animals likely in the range of 0-10 individuals per cell. We developed a spatially explicit sampling scheme for remote camera deployment. The sampling design considered habitat, access and historic information on ungulate density to determine where to place cameras.

We implemented a field trial at two study sites across two years (2015 and 2016), in two study sites each year, an open-habitat site (Beaverhead Zone) and a closed-canopy site (Panhandle Zone). We developed a power analysis to examine the number of cameras needed for this study. Field sites for the second season were selected in coordination with IDFG deer and elk inventory flights and with input from the area wildlife managers and researchers. We considered three potential analysis methods for those data based on animal detections in a time lapsed sampling scheme. The tested methods were instantaneous sampling, space-to-event, and finally, time-to-event analyses for camera data such as the REM model (Rowcliffe et al. 2008, Bishcof et al. 2013).

We hired an M.S. student in the Wildlife Biology Program at the University of Montana to perform this research, supervised by Dr. Paul Lukacs. The student worked closely with wildlife managers and researchers at IDFG during project development and field implementation.

In FY18, we extended the models developed by the M.S. student in FY17 to include estimators for herd composition of elk, mule deer, and white-tailed deer from camera trapping data. We also examined methods for estimating survival from camera data with unmarked animals using the time-series of the change in ratio detected by the cameras throughout the period from 1 week

after birth to January 1. We evaluated the models with aerial survey data performed near January 1.

In FY19 we developed sampling designs for remote camera composition, survival, and abundance estimates for deer and elk in several areas of the state of Idaho. Remotely triggered cameras provide large quantities of information about wildlife populations. Following our successful development of the theory and techniques to estimate demographic parameters from cameras, IDFG would like to efficiently integrate these techniques into ungulate management programs. Yet, the cameras are labor intensive to operate, cameras are expensive to purchase, and photo review is time consuming. Therefore, it is important to understand sampling design to aid in implementation of camera-based studies.

Sample size for camera studies involves several components. First, the number of cameras provides a spatially replicated sample of the environment. Second, the length of time a camera is operating in the field provides a temporal replicate of the camera location. Third, the number of observations of animals provides information about detection and abundance. The three components create a tradeoff in cost, effort and precision. Precision varies with each of the design components. Precision will increase when more cameras are used, but camera purchase and deployment costs will increase also. Precision will increase as cameras are deployed for a longer time, but bias may arise if animal distributions shift outside of the camera sampling area. Finally, precision will increase to some extent as the number of cameras increases, but the limits for that increase are unknown at this point. In addition to camera design considerations, animal density and movement rate influence the utility of different camera arrangements. Animals that occur at higher densities or move faster may be detected more frequently than rare or slow animals. Therefore, animal density and movement must be considered.

We examined the tradeoffs among camera design axes (numbers of cameras, duration and number of detections) in the face of varying animal density and movement rates. We examined the Space-To-Event and instantaneous sampling estimators to determine minimum camera sampling designs. For populations that fall below reliable density for STE, we examined Time-To-Event models that require information about movement. Following the determination of the optimal sampling design, we designed site-specific surveys for deer (Caribou population management unit) and elk (Panhandle and Elk City Zones). IDFG management personnel implemented the deployment and retrieval of cameras according to our design and protocol.

### ***Geographic Location***

Cameras were deployed in GMUs 6, 10A, 30, 30A, 69, 72, and 76 (Clearwater, Shoshone, Benewah, Lemhi, Bonneville, Bingham, Caribou, and Bear Lake counties).

### ***Principal Investigator(s)***

Mark Hurley (IDFG Wildlife Research and Data Manager)	208-287-2891
Jon Horne (IDFG Senior Wildlife Research Biologist)	208-799-5010
Paul Lukacs (University of Montana)	
Anna Moeller (University of Montana)	

Josh Nowak (Speedgoat Inc.)

### ***Timeline***

- Develop draft study plan: Oct - Dec 2014
- Field season 1: Jan - Mar 2015
- Data summation and preliminary analysis: Apr - Dec 2015
- Develop final study plan: Dec 2015
- Field season 2: Jan - Mar 2016
- Data analysis and thesis preparation: Apr 2016 - Jan 2017
- Manuscript preparation and submittal: Feb - Jun 2017
- Survival and ratio model and software development: July 2017 – April 2018
- Optimal sampling design and implementation: July 2018 – June 2019

### ***List of Partners***

University of Montana

### ***Results***

*Camera-based Abundance Estimation* - The graduate student on the project, Anna Moeller, developed and defended her MS thesis at the University of Montana. She developed three novel methods to estimate abundance of unmarked animals, including an Instantaneous Sampling (IS) estimator, a Time-to-Event (TTE) model, and a Space-to-Event (STE) model. Her thesis is available through the University of Montana at <https://scholarworks.umt.edu/etd/10958/>. She also published her research findings in the journal *Ecosphere* (Moeller et al. 2018).

To test these methods in the field, we completed one pilot season in winter 2014-15 and one full field season in winter 2015-16. We hired and led a crew of technicians to deploy 160 cameras near Salmon and St. Maries, Idaho in the winter of 2015-16 (Figure 1). We analyzed over 1.3 million pictures, including over 90,000 photos of elk and over 26,000 photos of mule deer. The methods produced realistic estimates in both study areas. In the Beaverhead Zone, estimates were similar to past aerial surveys and in the Panhandle Zone they fell within reasonable expectations. These represented the first abundance estimates for the Panhandle Zone.

We also formatted the models for Bayesian implementation in PopR to make them accessible to Idaho's managers and developed a theoretical model based on the STE model to concurrently estimate survival and abundance from cameras.

$$\begin{aligned} Y_i &\sim \text{Exp}(\lambda_i) \\ \lambda_i &= \lambda_{i-1} \cdot S \\ N_i &\sim \text{Pois}(\lambda_i) \cdot P \end{aligned}$$

We simulated data to test this model. By knowing “true” survival and abundance, we were able to show that the survival model produced unbiased estimates of survival and abundance (Figure 2). This model also allows managers to calculate calf:cow ratios from cameras. Ratios are based

on adult and juvenile survival and abundance, so they can be derived from the results of this model.

We used simulations and data collected during field work to explore sample size considerations for camera surveys employing the STE estimator. We examined how precision of the abundance estimate (measured with coefficient of variation) varied as a function of the number of cameras deployed. We also examined how precision and bias are affected by changing animal density with different levels of effort.

Sample size for camera trapping studies consists of a combination of the number of cameras placed in the field, the duration of time the cameras are set, and the number of target animals detected. The number of cameras deployed is the single most important component of sample size. The coefficient of variation or abundance drops as the number of cameras increases following a standard square root curve (Figure 3). Precision also declined as animal density decreased (Figure 4). At low density (1 animal per square km), only 4-10 detections of animals occurred with 50 cameras and 8-20 with 100 cameras. Despite these small numbers of detections, the model continued to provide unbiased estimates and precision remained reasonable for 100 cameras (Figure 4).

Animal distribution across the landscape has the potential to impact estimation and survey design as well. Therefore, we simulated a patchy distribution (overdispersed) to evaluate the effect of non-random mixing of animals in space. In field applications, patchy distributions of animals result in some cameras getting repeated observations of animals and some cameras getting few to no observations. The STE model assumes a Poisson distribution of animal numbers in the camera viewshed. Variation in the Poisson distribution is equal to the mean of the distribution which can be a limiting assumption in wildlife surveys. Therefore, we simulated data with variation up to 5 times greater than expected under a Poisson distribution. Estimated abundance remains unbiased in the presence of overdispersion at all levels tested. Theoretical standard errors under-estimated sampling variation as overdispersion increased, but bootstrapped standard errors captured the extra uncertainty (Figure 5). Moreover, the increase in realized uncertainty follows the square root of the magnitude of overdispersion as would be theoretically expected.

We used these results to develop recommendations for camera sample sizes per stratum (Table 1), survey duration, and camera placement when using the STE model to estimate ungulate abundance. Rows of Table 1 represent varying levels of precision from a CV of 10%-50%. Columns of Table 1 represent varying levels of animal patchiness. We used elk distribution in the Beaverhead winter range as a reference level of elk distribution. If the target study area is thought to have elk clumped in groups twice as variable as the Beaverhead, then camera numbers in the "2x" column should be considered for the survey design. We rounded all numbers of cameras up to the next multiple of 25 for simplicity in design recommendations.

The duration of a camera survey should be at least as long as the animals are present on winter range and migratory behavior is minimized. Beyond that consideration, time stamps on photos allow survey period to be determined at the analysis stage. STE model assumes random placement of cameras with no lure, bait, or attractant. As a practical consideration, selecting a grid cell at random and placing a camera subjectively within that cell seems to be a reasonable

approach. In more open habitat, such as sagebrush, large cell sizes can be used because ungulates use the landscape more evenly. In more closed habitat, cell size must be smaller to guard against subjective placement only on actively used trails. At this time, we recommend 30m cells for closed forest habitats and 200m cells for open sage brush. Additional testing of cell size would be useful in the future.

Managing and analyzing the millions of pictures produced from these sampling efforts remains a logistical problem. Therefore, we also collaborated with other researchers to examine methods to use machine learning models to automatically separate pictures that do and don't contain animals and classify pictures by the wildlife species they contain (Tabak et al. 2018). The model classified approximately 2,000 images per minute with 94% accuracy on whether the image contained an animal or not and >82% accuracy on species identification. The continued development of this technology will facilitate wide use of remote camera estimation methods.

Based on these accumulated results, we developed a sampling design and protocols for camera placement and field deployment of cameras to estimate elk and mule deer abundance. We developed resource selection functions (RSF) from locations collected from GPS-collared elk in GMUs 6 and 10A and mule deer in the Caribou population management unit (PMU; GMUs 69, 72, and 76) to predict winter distribution of animals. We generated 150 random locations within the modeled winter distribution at each study site (GMU 6, GMU 15, and Caribou) for camera placement. IDFG management personnel executed the sampling design we developed and deployed and retrieved cameras. Picture processing and analyses from these cameras is ongoing. The mule deer abundance estimate generated in the Caribou PMU will be compared to an estimate generated from traditional sightability aerial survey conducted in winter 2018-19 as a form of validation.

*Camera-based Estimation of Neonate Survival* - The data consist of pictures taken from an array of motion-triggered camera traps (CT) which are deployed on the landscape. Observed data are a record of the number of female adults ( $y_{a,T}$ ) and neonates ( $y_{n,T}$ ) in a picture, or set of pictures, taken at time  $T$  from just before neonates start showing up in pictures though the end of the observation period. To estimate neonate survival, we model the observed picture data as a function of the neonate survival process while taking into account other processes (biological, behavioral, and observational) that affect the number of neonate and adult photographs. We begin by assuming that the number of neonates photographed is a binomial random variate, with probability  $\phi_{n,T}$  that the individual is a neonate and sample size equal to the total number of photographed individuals ( $y_T = y_{n,T} + y_{a,T}$ ):

$$y_{c,T} \sim \text{Binomial}(\phi_{n,T}, y_T). \quad \text{eqn 1}$$

We then recognize that  $\phi_{n,T}$  is a function of the ratio of the actual number of neonates ( $N_{n,T}$ ) to female adults ( $N_{a,T}$ ) in the study area and their respective detection probabilities,  $d_{n,T}$  and  $d_{a,T}$

$$\phi_{n,T} = 1 - \left[ 1 + \frac{N_{n,T} \times d_{n,T}}{N_{a,T} \times d_{a,T}} \right]^{-1}. \quad \text{eqn 2}$$

Next, we decompose eqn 2 into the biological processes that determine the abundance of female adults and neonates. The expected number of female adults at time  $T$  is the number at the beginning of the observation period ( $T = 0$ ) multiplied by the probability of surviving to  $T$

$$N_{a,T} = N_{a,0} \times S_a(T). \quad \text{eqn 3}$$

Because the observation period will include the time before and after neonates are born, the expected number of neonates at time  $T$  is a function of (1) the number of female adults, (2) the parturition rate of female adults, (3) the distribution of neonate birth dates, and (4) the neonate survival function. Thus,

$$N_{n,T} = \int_{t=0}^T [N_{a,t} \times R \times b(t)] \times [S_n(T-t)], \quad \text{eqn 4}$$

where  $R$  is the reproductive rate (i.e., expected number of young born to each female),  $b(t)$  is a function describing the probability density that an individual is born at time  $t$ , and  $S(z)$  is a function describing the probability of surviving  $z$  time units. Henceforth, we use  $z = T - t$  to represent the age of the neonate. The first bracketed term in eqn 4 is the expected number of neonates born at time  $t$  and the second bracketed term is the expected proportion of neonates born at time  $t$  that survive to  $T$ . Combining eqn 2, 3, and 4 we have

$$\phi_{n,T} = 1 - \left[ 1 + \frac{\int_{t=0}^T N_{a,0} \times S_a(t) \times R \times b(t) \times S_n(z) \times d_{n,T}}{N_{a,0} \times S_a(T) \times d_{a,T}} \right]^{-1}. \quad \text{eqn 5}$$

The probabilities that an individual is photographed ( $d$ ) in eqn 5 are the last components to connect our picture data to the neonate survival process. For the neonate detection probability we recognize that for most animals there is a “hiding” phase where the mobility of the newborn neonate is restricted substantially compared to female adults, but over time as the neonate ages and becomes more mobile, it will eventually acquire mobility similar to that of the maternal adult. Thus, we suggest modeling  $d_{n,T}$  as a combination of two probabilities: the probability that a neonate is available (e.g., mobile enough) to have a picture taken  $a(z)$  and given that it is available, the probability that an actual photo is acquired ( $p_T$ ). Thus,  $d_{n,T} = a(z) \times p_T$ , where  $a(z)$  is a function describing the cumulative probability over time that a neonate of age  $z$  is available (i.e., mobile) to be photographed. For female adults, we assume that they have the same probability of being photographed at time  $T$  as neonates when  $a(z)=1$ . Thus, our final model for the probability of obtaining a neonate picture, after moving appropriate terms outside of the integral, is

$$\phi_{n,T} = 1 - \left[ 1 + \frac{R \times p_T \times N_{a,0} \int_{t=0}^T S_a(t) \times b(t) \times S_n(z) \times a(z)}{p_T \times N_{a,0} \times S_a(T)} \right]^{-1} \quad \text{eqn 6}$$

After cancelling terms,

$$\phi_{n,T} = 1 - \left[ 1 + \frac{R \int_{t=0}^T S_a(t) \times b(t) \times S_n(z) \times a(z)}{S_a(T)} \right]^{-1} \quad \text{eqn 7}$$

Substituting eqn 7 into eqn 1 allows us to model the observed picture data as a function of the neonate survival process and estimate the associated parameters. In practice, the integral in eqn 3 will be intractable, so we approximate it by discretizing time (e.g.,  $t$  = daily time steps) and summing over  $t$ . Thus, our observed number of neonate and female adult pictures are a function of 5 processes: the female survival function, the reproductive rate of adults, the distribution of birth dates, the distribution of when neonates are available for photographs, and the neonate survival function. It is apparent from eqn 7 that some of these processes are confounded and CT data alone cannot estimate the parameters associated with all of these functions. But with some prior information, we were interested in whether CT data could be used to estimate the neonate survival function.

A few important properties of eqns 6 and 7 emerge. First, the probability of an individual being photographed at time  $T$  ( $p_T$ ) cancels out from eqn 7. Thus, a parameter that can be difficult to estimate for most field implementations of CTs, is not needed with far reaching implications. For example, individual CTs can have an unknown, undocumented or changing view shed during the study. Similarly, the probability of detection can change over space and time. For example, cameras can be added, taken down, adjusted, or moved during a study; or, animal movements and space use can make individuals more or less detectable during some periods than others. Additionally, CTs do not need to be placed independent of animal density (i.e., randomly) and can intentionally be placed in areas presumed to maximize the number of photos, a design that will increase the precision of the survival estimate but also allow cameras to be used for other purposes (e.g., documenting occurrence of rare and elusive animals). Related to  $p_T$  cancelling out, we do not need to know or estimate the abundance ( $N$ ) of neonates or adults in the study area. While methods for abundance estimation from CTs for unmarked individuals is progressing, it remains difficult to implement these methods either from the standpoint of meeting critical assumptions or adhering to stringent sampling designs.

The considerations discussed above allow researchers substantial freedom in placing cameras on the landscape, with some caveats. For valid inference, CTs should be placed such that spatial distribution is representative of the target population for which inferences are to be made. If the purpose of the deployment is to maximize precision of the survival estimate, CTs should be placed to maximize the number of animal pictures (e.g., game trails). However, when deploying CTs there is one critical assumption that must be carefully considered. We assumed that once neonates are available for being photographed, they have the same probability that a photo is

taken as female adults. In reality, most mammalian neonates stay in close proximity to their maternal adult for an extended period of time. Thus, we can assume there are generally two groups on the landscape, females without neonates and females with neonates. For our model to be unbiased, we assume that these two groups have the same probability of detection. For example, in our simulations we assumed that females with and without neonates have the same probability of being available for a photo (i.e., in the area of the CT) and then given an adult female in the area, each individual (female with neonate(s), female without neonate(s), and the neonate) has the same probability that an actual photo is taken. If there are substantial differences in space use between females with versus without neonates, CTs should be placed such that both groups have a similar probability of detection. Additionally, CTs should be placed with a viewshed that does not inhibit viewing neonates (e.g., tall grass that might hide a neonate while adults are visible) or triggering the motion sensor (e.g., detection zone too high).

Our model assumes that female adults and neonates are identified without error. This assumption puts a limit on the duration of the study because as neonates age, they become more difficult to distinguish from adults. Truncating the study period before neonates become hard to separate from adults will prevent misclassification of neonates which will subsequently bias survival estimates low. Our model is best suited for species that have a birth pulse (e.g., annual) as this will provide a cohort of neonates that can be easily distinguished from adult females. Regarding identification of adult females, for many field implementations this group will include individuals that are approximately 1 year old. Thus, the parturition rate ( $R$ ) should include individuals that were  $< 1$  year old during the previous breeding season.

We did not specify the specific functions that should be used for adult female survival  $S_a(\cdot)$ , the distribution of birth dates  $b(t)$ , the time-to-availability function for neonates  $a(z)$ , or neonate survival  $S_n(z)$  as these functions should be chosen based on the biology of the particular species under investigation. Because we are using relatively limited data (i.e., the ratio of adult female to neonate pictures) to provide information on several processes, these functions should be relatively simple to keep the number of parameters that need to be estimated as small as possible while still providing useful information. In subsequent sections we describe and provide justification for the functions we used for implementing the model with North American elk (elk, hereafter; *Cervus canadensis*). Even with simple functions, there will not be enough information in CT data alone to estimate all of the associated parameters, as some are obviously confounded (e.g., adult female versus neonate survival). Thus, some of the parameters will need to be estimated *a priori* and provided as prior information. As it was not obvious how the model would respond to various levels of prior information, we used simulations to investigate potential bias and parameter identifiability under varying amounts of prior information.

We used simulated data with elk in the northern Rocky Mountains, U.S.A. as an example species. We briefly describe these simulations. Adult female elk generally give birth in spring ( $\sim$  early June; citation) and neonates can easily be distinguished from adults throughout the summer and into the fall, thus, we generated data from 1 May to 15 October (167 days). We started with an initial population of 400 adult ( $\geq 1$  year old) females and simulated 300 replicate datasets. Elk rarely give birth to  $\geq 1$  calf (Hudson and Haigh 2002), therefore, for each dataset we assigned whether each female was pregnant by drawing a Bernoulli variate with probability equal to 0.5. Adult females generally have relatively high and constant survival throughout the

summer until hunter harvest begins in fall so each adult female was assigned a survival time by drawing a random deviate from an exponential survival model  $f(t) = \lambda \exp(-\lambda t)$  with a constant hazard of death  $\lambda = .0003$ . Each adult female that was pregnant was assigned a parturition date ( $PD$ ) by drawing from a random deviate from a lognormal distribution  $PD \sim \text{lognormal}[\mu, \sigma^2]$  with  $\mu = 3.6$  and  $\sigma = 0.3$ , corresponding to a mode on 2 June and a standard deviation equal to 12. Calves were born to adult females that survived longer than the parturition date. Each calf was assigned a survival time by drawing a random deviate from a Weibull distribution with shape parameter ( $\alpha$ ) and scale parameter ( $\beta$ ). To investigate our model performance for a range of potential survival functions, we reparametrized the Weibull distribution in terms of the overall survival rate for the observation period ( $S_{167}$ ) using  $\beta = 167 / -\ln S_{167}^{1/\alpha}$  and simulated 9 alternative survival functions (Figure 6) derived from 3 levels of the shape parameter ( $\alpha = 0.3, 0.65, 1$ ), and 3 levels of the ~5.5 month survival rate ( $S_{167} = 0.7, 0.5, \text{ and } 0.3$ ). Each calf was assigned a time-to-availability (i.e., the time until a calf was mobile enough to be exposed to a CT) by drawing a random deviate from a Weibull distribution with shape parameter  $\gamma = 3$  and scale parameter  $\delta = 12$ . For each adult female (with and without a neonate), we drew series of random times when they were within the CT detection zone from an exponential distribution where the daily detection rate = 0.1. Once an adult female was in the detection zone, a picture was taken with probability equal to 0.9. Neonates whose maternal adult was in the detection zone had a picture taken with probability equal to 0.9.

From the steps above, each individual cow and calf has a picture history of times when a picture was taken. For the integral in eqn 7, we used daily time steps and summed the total number of individuals in pictures ( $y_T$ ) and the number of neonates in pictures ( $y_{c,T}$ ) each day. These were the data for a binomial trial (eqn 1). We fit the model using Bayesian Markov chain Monte Carlo (MCMC) methods in Program R (version 3.3.1; R Foundation for Statistical Computing, Vienna, Austria) using JAGS (version 3.4.0; Plummer 2003) and the R package JagsUI (version 1.1). We ran 6 MCMC chains for 10,000 iterations, used 500 for the adaptive phase and 5,000 as burn-in. For each of the 300 replicate datasets, we determined the mode of the posterior distributions and used that as the estimate of the overall survival rate of neonates ( $S_{167}$ ) and shape of the survival function ( $\alpha$ ).

In addition to the neonate survival function, our elk model has 4 processes and 6 associated parameters (Table 2). We anticipated that some or all of these additional parameters would have to be estimated *a priori* and provided as either known values or informative priors. We investigated which parameters could be reliably estimated with CT data by progressively adding unknown processes to the estimation procedure and monitoring potential bias in the estimates of neonate survival function. For our simulations, we provided *a priori* parameters as known values that equaled the true value that generated the simulated data. We considered our model to be an unbiased estimate of the neonate survival function if the mean of the estimated survival function across the 300 replications was within +/- 0.05 of the true value.

Estimates of the summer survival rate ( $S_{167}$ ) and the shape of the survival function ( $\alpha$ ) were unbiased when the neonate availability process alone was estimated as well as when the neonate availability processes was estimated (Table 2, Figure 7a and 7b). When all 3 processes were

estimated (i.e., neonate survival, availability and distribution of birth dates), the estimate of  $S_{167}$  was unbiased but the estimate of  $\alpha$  was biased high which resulted in estimates of mid-summer survival being overestimated by ~5 - 10% (Table 2, Figure 7c).

Based on the results of the simulations we began field implementation in the summer of 2019. We deployed 89 research cameras in Unit 10A in June 2019 to collect data for estimating elk calf survival. The study area was divided into 145 1.5x1.5 km cells (approximately 1 square mile). Cells that contain a camera were selected using a spatially balanced random sampling procedure (i.e., Generalized Random Tessellation Sampling; GRTS). Cameras were placed at locations that are deemed to have the highest probability of capturing elk photos at both the local scale (e.g., heavily used game tails) and more generally (e.g., preferred slope, topographic position, habitat, etc.). Cameras will be deployed with lithium batteries which, based on previous camera deployments in GMU 16, should last for at least 1 year.

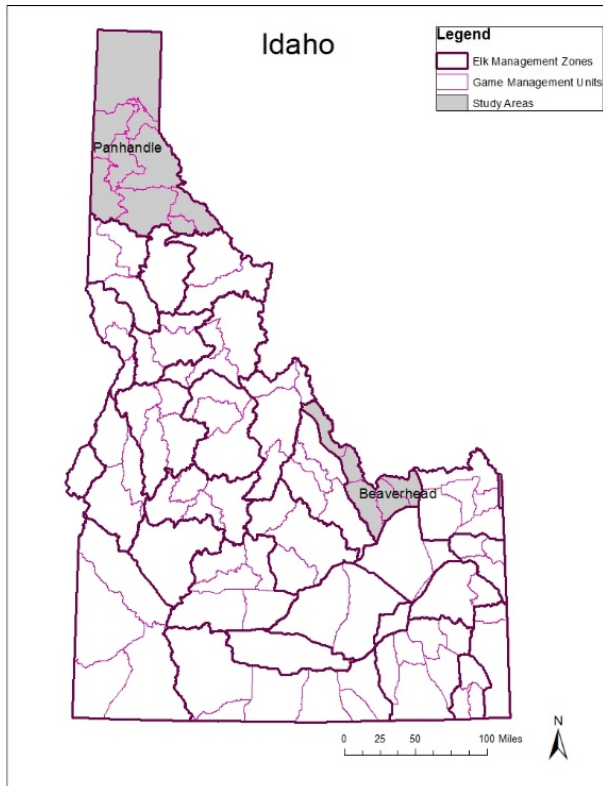
**Table 1.** Recommended numbers of cameras for varying target levels of precision and patchiness of animal distributions. The 20% row is highlighted because it represents a reasonable balance between effort and information gain.

Precision (%CV)	Patchiness relative to Beaverhead elk winter range				
	Similar	2x	3x	4x	5x
10	150	175	200	250	300
20	100	150	175	200	250
30	75	100	150	175	200
40	50	75	100	150	175
50	50	50	75	100	150

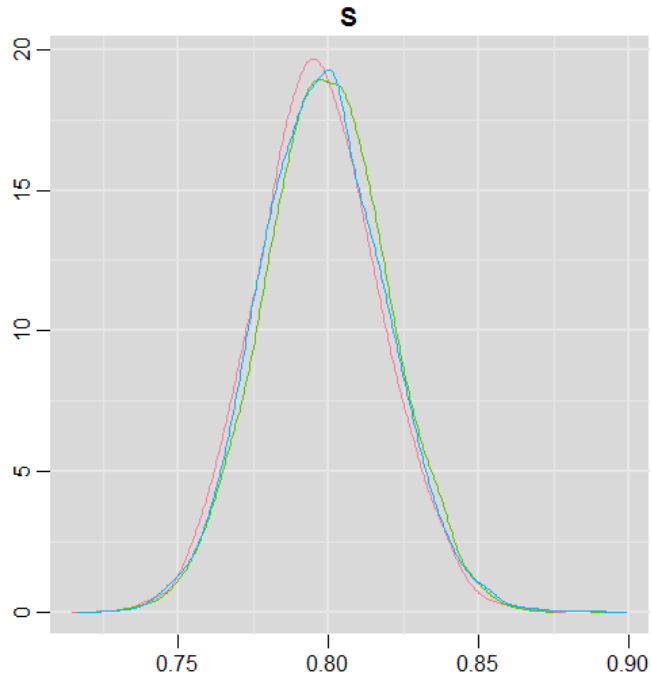
**Table 2.** Processes, functions, and associated parameters used in an elk neonate survival model based on remote camera trap data.

Biological process	Function	Parameters	Estimate with CT data
Neonate survival	Weibull	$S_{167}, \alpha$	Unbiased
Neonate availability	Weibull	$\gamma, \delta$	Unbiased
Neonate birth date	Lognormal	$\mu, \sigma$	Biased

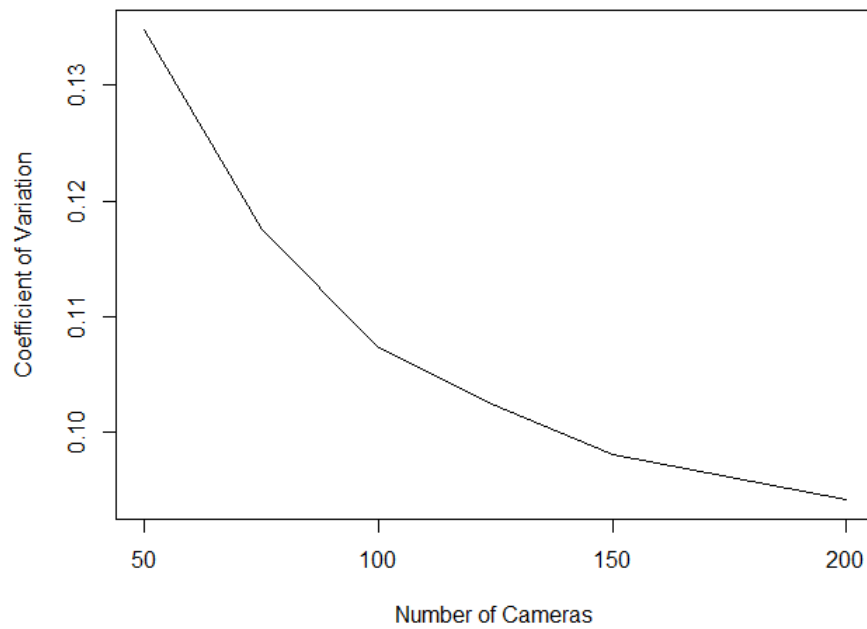
**Figure 1.** Camera trapping test study areas.



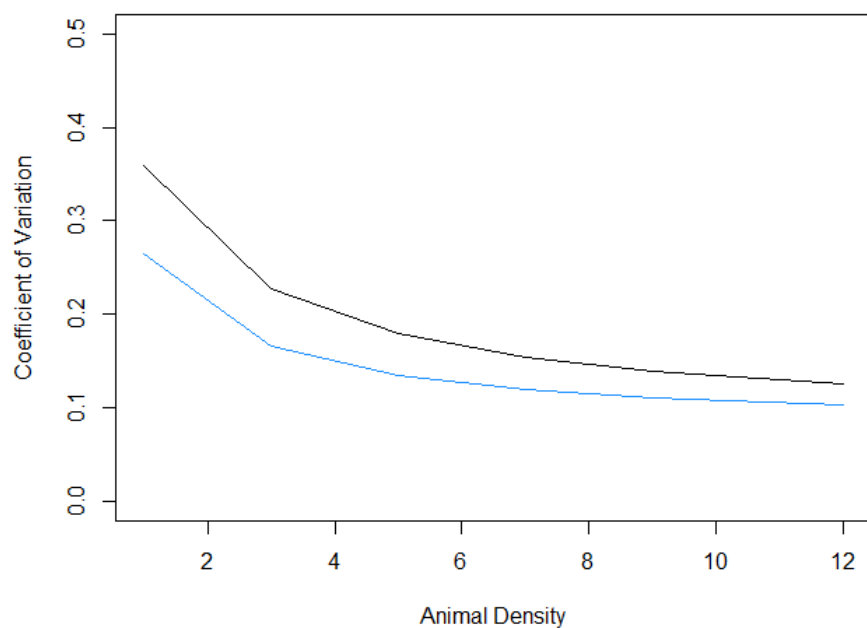
**Figure 2.** Results from estimating survival from simulations. The three chains converged on the true value of survival (0.80).



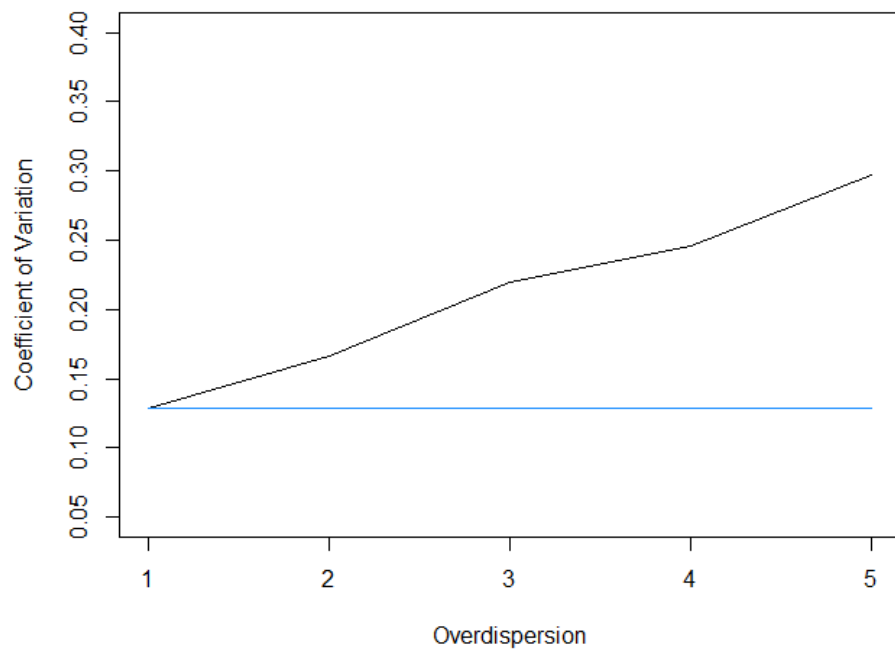
**Figure 3.** Precision of estimated abundance (coefficient of variation) as a function of the number of cameras deployed in a survey.



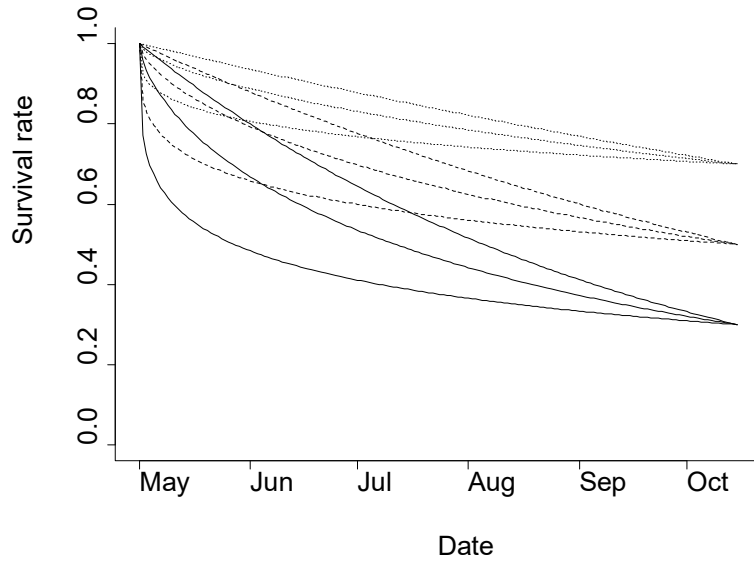
**Figure 4.** Precision of estimated abundance (coefficient of variation) as a function of animal density (animals per  $\text{km}^2$ ) and number of cameras (black line = 50 cameras, blue line = 100 cameras).



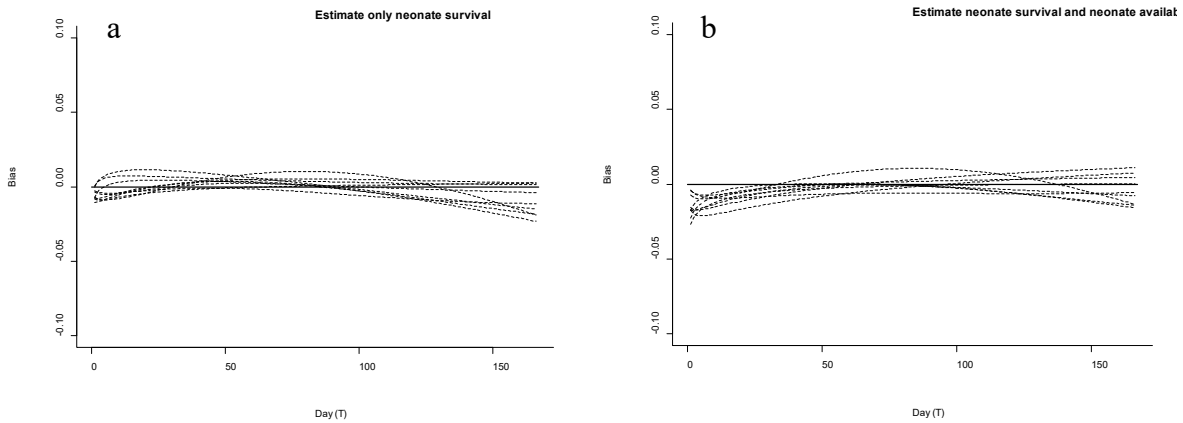
**Figure 5.** Precision of estimated abundance (coefficient of variation) as a function of extra Poisson variation (overdispersion). Values of overdispersion represent multiples of the mean parameter of a Poisson distribution. Theoretical CV is presented in blue and bootstrap CV is presented in black.

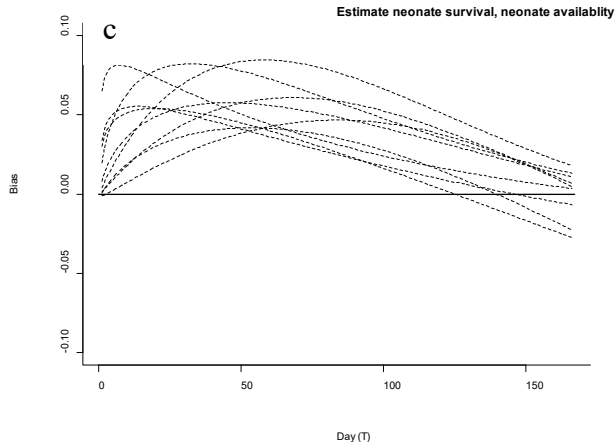


**Figure 6.** Elk neonate survival functions used in simulations to evaluate the performance of our model.



**Figure 7.** Bias in the estimated neonate survival function when only neonate survival was estimated and all other model parameters were provided (a), when the neonate survival function and the neonate time-to-availability process was estimated (b), and when the neonate survival function, the neonate time-to-availability process, and the distribution of neonate birth dates was estimated (c).





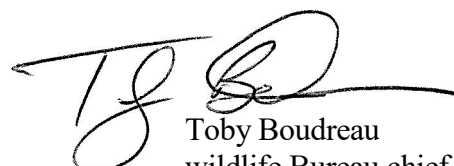
## Literature Cited

- Bischof, R., et al. 2014. Using time-to-event analysis to complement hierarchical methods when assessing determinants of photographic detectability during camera trapping. *Methods in Ecology and Evolution* 5: 44-53.
- Moeller, A. K., P. M. Lukacs, and J. S. Horne. 2018. Three novel methods to estimate abundance of unmarked animals using remote cameras. *Ecosphere* 9(8):e02331. 10.1002/ecs2.2331
- Rowcliffe, J. M., et al. 2008. Estimating animal density using camera traps without the need for individual recognition. *Journal of Applied Ecology* 45: 1228-1236.
- Tabak, M. A., M. S. Norouzzadeh, D. W. Wolfson, S. J. Sweeney, K. C. Vercauteren, N. P. Snow, J. M. Halseth, P. A. Di Salvo, J. S. Lewis, M. D. White, B. Teton, J. C. Beasley, P. E. Schlichting, R. K. Boughton, B. Wight, E. S. Newkirk, J. S. Ivan, E. A. Odell, R. K. Brook, P. M. Lukacs, A. K. Moeller, E. G. Mandeville, J. Clune, and R. S. Miller. 2018. Machine learning to classify animal species in camera trap images: applications in ecology. *Methods in Ecology and Evolution* 2018:1-6. 10.1111/2041-210X.13120

Submitted By:

Mark Hurley, Wildlife Research Manager  
[Mark.hurley@idfg.idaho.gov](mailto:Mark.hurley@idfg.idaho.gov)

  
 Martha Wackenhut  
 Federal Aid Cooreinator

  
 Toby Boudreau  
 wildlife Bureau chief